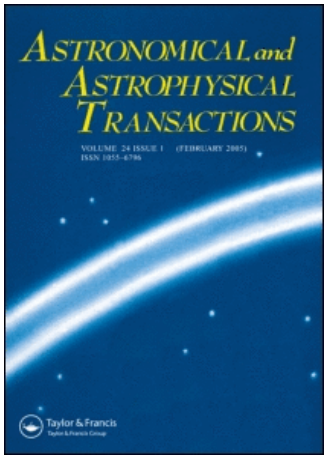

Astronomical & Astrophysical Transactions
The Journal of the Eurasian Astronomical Society
Publication details, including instructions for authors and subscription information:
http://www.informaworld.com/smpp/title~content=t713453505

Analysis of the broad emission line profiles in the active galactic nucleus 3C 390.3

L. S. Nazarova [a]; N. G. Bochkarev [b]; C. M. Gaskell [c]
[a] Euro-Asian Astronomical Society, Universitetskij Prospekt 13, Moscow, Russia
[b] Sternberg Astronomical Institute, Universitetskij Prospekt 13, Moscow, Russia
[c] Department of Physics and Astronomy, University of Nebraska, Lincoln, Nebraska, USA

Online Publication Date: 01 August 2004
To cite this Article: Nazarova, L. S., Bochkarev, N. G. and Gaskell, C. M. (2004) 'Analysis of the broad emission line profiles in the active galactic nucleus 3C 390.3', Astronomical & Astrophysical Transactions, 23:4, 343 - 352
To link to this article: DOI: 10.1080/10556970410001729544
URL: http://dx.doi.org/10.1080/10556970410001729544

Astronomical and Astrophysical Transactions
Vol. 23, No. 4, August 2004, pp. 343–352

ANALYSIS OF THE BROAD EMISSION LINE PROFILES IN THE ACTIVE GALACTIC NUCLEUS 3C 390.3

L. S. NAZAROVA[a], N. G. BOCHKAREV[b] and C. M. GASKELL[c]

[a]*Euro-Asian Astronomical Society, Universitetskij Prospekt 13, Moscow 119899, Russia;* [b]*Sternberg Astronomical Institute, Universitetskij Prospekt 13, Moscow 119899, Russia;* [c]*Department of Physics and Astronomy, University of Nebraska, Lincoln, Nebraska 68588-0111, USA*

(Received 17 September 2003)

We present a study of ultraviolet and optical spectra of the active galaxy 3C 390.3 taken as part of the International Active Galactic Nuclei (AGNs) Watch during the period January 1995–January 1996. We have measured the C IV-to-Lyα and Lyα-to-Hβ ratios at different velocities in the line profiles. We find that the Lyα-to-Hβ ratio varies across the line profiles. The ratio is high in the low-velocity centre of the lines at all times but decreases in the high-velocity wings. The C IV-to-Lyα line ratio, however, is low at the line centre but becomes higher in the wings. This velocity dependence of line ratios is different from what has been reported for most other AGNs. Theoretical modelling of the C IV-to-Lyα and Lyα-to-Hβ ratios, using the photoionization code CLOUDY, suggests that the density is higher in the higher-velocity gas producing the displaced broad line peaks, and that the observed line ratios can be accounted for by two systems of clouds. One corresponds to a high ionization line zone with an electron density, $N_e \approx 10^{10}$–10^8 cm^{-3}. It is presumably located above the accretion disc. The other system corresponds to a low-ionization line zone which, because of the line profiles, is probably part of the accretion disc, and which has a higher electron density, $N_e \approx 10^{11}$–10^{12} cm^{-3}. We discuss the possible geometry of the broad-line-region in 3C 390.3.

Keywords: Active galaxy 3C 390.3; C IV-to-Lyα ratio; Lyα-to-Hβ ratio; Emission line profiles

1 INTRODUCTION

One of the major problems in active galactic nuclei (AGNs) research has been the nature and origin of the broad emission lines. These lines differ from lines produced by more familiar H II regions ionized by stars in that a very wide range of ionization is seen. Some of these lines, such as C IV and Lyα, arise from a highly-ionized hydrogen zone, and we shall refer to these as 'high-ionization lines' (HILs); other lines, including the bulk of the Hβ emission, arise from a large warm, partially-ionized zone, and we shall refer to these as 'low-ionization lines' (LILs). The nature of the regions producing these two types of line is an unsolved question.

The emission lines of AGNs vary in response to changes in the extreme ultraviolet (UV) and soft-X-ray flux (Bochkarev and Pudenko, 1975). Monitoring the time variability of both the emission lines and the continuum is an excellent approach for investigating the innermost region of AGNs (Blandford and McKee, 1982; Antokhin and Bochkarev, 1983). AGN 3C 390.3 was monitored in both the optical and the UV during the period 1994–1996 as part of a monitoring

* Corresponding author. E-mail: gaskell@unlserve.unl.edu

ISSN 1055-6796 print; ISSN 1476-3540 online
DOI: 10.1080/10556970410001729544

campaign by the International AGN Watch (IAW). The observational data for both regions of spectra are available now for the astronomical community in the IAW archives.

3C 390.3 is a Fanaroff–Riley type II (FR II) radio galaxy at a red shift $z = 0.056$, with a 60″ one-sided narrow jet at a position angle of $-37°$. The Balmer lines have localized peaks that are displaced to substantially higher and lower velocities than the narrow lines (Sandage, 1966). The AGN 3C 390.3 is the prototype of the class of AGNs showing complex broad-line profiles with displaced peaks (Gaskell, 1983). The line profiles of 3C 390.3-type objects suggest highly ordered velocity fields with highly structured gas distributions and/or an anisotropic illumination of the broad-line region (BLR).

Several models have been proposed to explain these line profiles. Most of these have sought a single explanation for the profiles and for their variations. The red and blue wings of the Balmer lines appear to vary independently on relatively long time scales (Zheng *et al.*, 1991), in conflict with the simplest disc models (Gaskell, 1988). However, on shorter time scales, the red and blue wings vary together (Dietrich *et al.*, 1998) as expected for disc models (Gaskell and Snedden, 1999).

In this paper we report the results of a profile study, at different states of nuclear activity, for the 'high-ionization' C IV and Lyα lines and also for the 'low-ionization' Hβ line. The paper is organized as follows: the observational data used for this study are described in Section 2; the results of the analysis of the line profiles are presented in Section 3; the photoionization modelling of the line ratio is discussed in Sections 4 and 5; conclusions are presented in Section 6.

2 OBSERVATIONAL DATA

The UV and optical spectra were taken from the IAW database for the period January 1995–January 1996. We show the UV light curve in Figure 1(a). We have chosen eight spectra

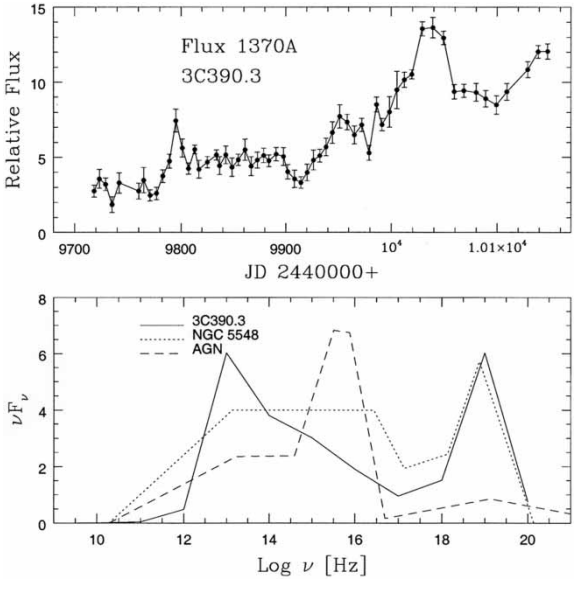

FIGURE 1 (a) The continuum light curve of 3C 390.3 at $\lambda = 1370$ Å. (b) The spectral energy distribution (SED) of 3C 390.3, together with the SED of NGC 5548, and the canonical Matthews and Ferland (1987) AGN continuum SED. The continua are plotted as νF_ν with arbitrary scaling.

TABLE I Log of spectroscopic observations.

File name	*Date*	*Julian date (2 400 000+)*	*Lines*
53651	24 January 1995	2 449 741.873	Lyα, C IV
53890	11 February 1995	2 449 760.255	Lyα, C IV
54049	6 March 1995	2 449 782.807	Lyα, C IV
56113	21 October 1995	2 450 012.226	Lyα, C IV
56158	7 November 1995	2 450 029.114	Lyα, C IV
56243	27 November 1995	2 450 049.144	Lyα, C IV
56304	16 December 1995	2 450 068.253	Lyα, C IV
56385	6 January 1996	2 450 088.975	Lyα, C IV
c49744db	27 January 1995	2 449 744.588	Hβ
c49770ee	22 February 1995	2 449 770.951	Hβ
c49779zze	3 March 1995	2 449 780.111	Hβ
c50051be	30 November 1995	2 450 051.623	Hβ
c50068be	17 December 1995	2 450 068.597	Hβ

in the UV region and five spectra in the optical region, taken at times of maximum and minimum luminosities. Details of these spectra are given in Table I.

The time lag between the continuum and the line flux for Hβ obtained from ground-based monitoring during 1994–1995 was 20 ± 8 days (Dietrich *et al*., 1998), and initially it appeared that this was greater than the time lags of lines arising in the low-ionization region (O'Brien *et al*., 1998; Dietrich *et al*., 1998). However, in a recent study of the optical spectra of 3C 390.3 for the period 1992–2000, Sergeev *et al*. (2002) found the lag between the continuum and Hβ emission line variations to be 89 ± 11 days. Sergeev *et al*. demonstrated that the differences between their lag and that of Dietrich *et al*. are probably due to sampling effects. Shapovalova *et al*. (2001), on the basis of long-term monitoring with the 6 m telescope of the Special Astrophysical Observatory, reported that the response time lag of Hβ relative to the (optical) continuum flux varied somewhat with time but was generally around 35–100 days. The time lags for the 'high-ionization' C IV and Lyα lines lie within this range (Wamsteker *et al*., 1997; O'Brien, 1998; O'Brien *et al*., 1998). O'Brien *et al*. (1998) obtained lags for the C IV and Lyα lines of 37 ± 14 days and 60 ± 24 days respectively.

3 ANALYSIS OF THE LINE PROFILES

We show line profiles around maximum and minimum activities in Figure 2. For our analysis we have divided the profiles of the C IV, Lyα and Hβ lines into seven equal velocity bins, the width of each part being $2000\,\mathrm{km\,s^{-1}}$. The core of the lines is measured between -1000 and $+1000\,\mathrm{km\,s^{-1}}$. Thus our highest-velocity blue and red bins extend out to $\pm 7000\,\mathrm{km\,s^{-1}}$. Note that the maximum of the blue-shifted peak located between -3000 and $-5000\,\mathrm{km\,s^{-1}}$ is measured separately from other parts of the wings (see Figure 2). The displaced blue peak in the low-ionization Hβ line is stronger than in the high-ionization lines C IV and Lyα at the minimum of nuclear activity (Figures 2(a), (c) and (e)). However, the blue peak in the HILs is more prominent during the maximum of nuclear activity (Figures 2(b), (d) and (f)).

Figure 3 shows the C IV-to-Lyα and Lyα-to-Hβ line ratios as functions of velocity for the minimum and maximum states of the nuclear activity. Two complications in our analysis must be mentioned. The first is the difficulty in removing the narrow-line region (NLR) component, especially in the UV lines, because of the poor wavelength resolution of the IUE satellite's

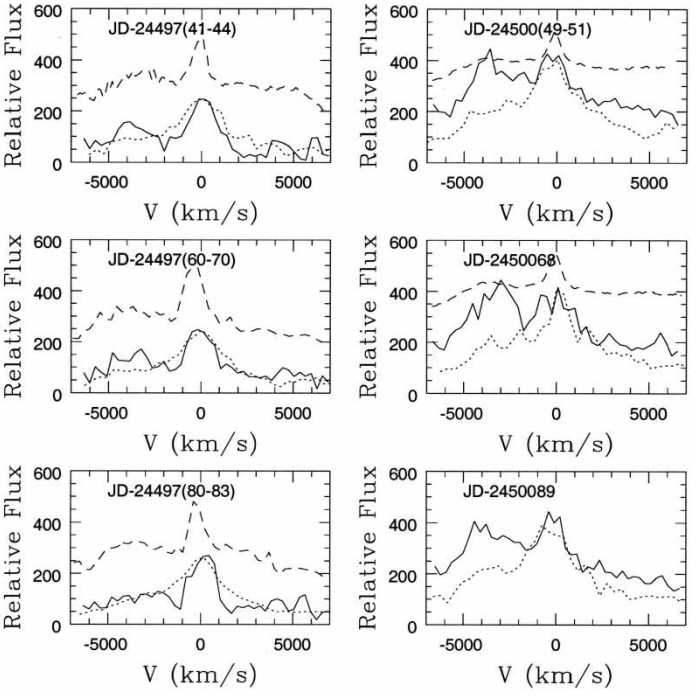

FIGURE 2 Line profiles during (a), (c), (e) minimum and (b), (d), (f) maximum states of activity: ———, C IV; · · · · · ·, Lyα; - - - - -, Hβ.

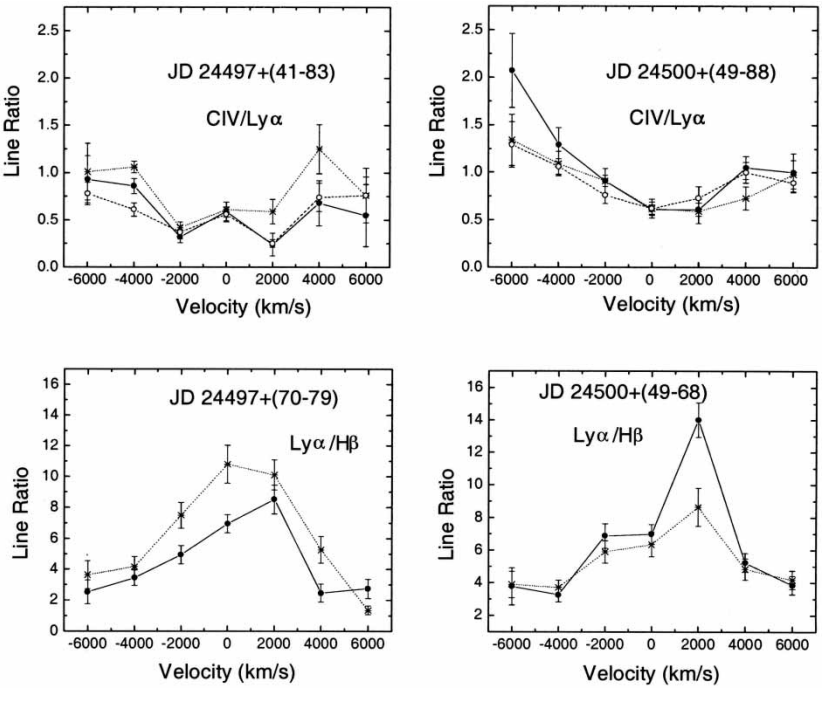

FIGURE 3 C IV-to-Lyα and Lyα-to-Hβ line ratios for (a), (c) the minimum and (b), (d) the maximum states of nuclear activity. The ratios shown by the solid lines are derived from spectra taken on JD 2 449 741, JD 2 449 770, JD 2 450 049, and JD 2 450 051. The ratios shown by the dashed lines are derived from spectra taken on JD 2 449 760, JD 2 449 779, and JD 2 450 068. The ratios shown by the dotted lines are derived from spectra taken on JD 2 449 783 and JD 2 450 088.

low-resolution spectrographs. As can be seen in Figure 2, there is a substantial NLR component in each line. However, inspection of Figure 3 shows that removal of the points at zero velocity does not change our results. The second complication is that in Figure 3 we have not attempted to make any corrections for reddening. Gaskell *et al*. (2004) have shown that the reddening curve in the UV for radio-loud AGNs is very flat, so the C IV-to-Lyα ratio will be completely insensitive to reddening. The Lyα-to-Hβ ratio, however, *is* strongly reddening dependent and, as it is now clear (Gaskell *et al*., 2004) that radio-loud AGNs such as 3C 390.3 are reddened, this must be taken into account in our analysis.

In the low state (Figures 3(a) and (c)), the NLR component is conspicuous in the zero-velocity bin; so this bin should be ignored. The NLR contamination is much less important in the high state. It can be seen from Figure 3 that the C IV-to-Lyα ratio is low in the low-velocity regions of the line profile but becomes higher in the wing, particularly when 3C 390.3 is more active. The asymmetry in the line ratios between the blue and red wings could be real, since the blue peak was stronger at this time, but it could also be an artifact of the extreme difficulty in removing NV 1240 Å emission from the wing of Lyα in an object with line profiles as complex as those of 3C 390.3.

The observed Lyα-to-Hβ ratio is high at low velocities and decreases in the wings for both high and low states of the nuclear activity. This velocity dependence is the opposite of what is seen for most AGNs (Snedden, 2001, Snedden and Gaskell, 2004b), where the Lyα line is usually broader than the Balmer lines. These differences imply somewhat different conditions in the regions producing the blue and the red wings.

4 PHOTOIONIZATION MODELS

To model the emission regions we used the photoionization code CLOUDY (version c90.05) (Ferland *et al*., 1998; 2004), using a plane-parallel geometry and solar abundances. We used the 3C 390.3 SED shown in Figure 1(b). We calculated models covering a range of electron density from 10^7 to 10^{13} cm^{-3}.

Since the observed luminosity and observed SED of 3C 390.3 are known, and since reverberation mapping gives the distance of the gas from the centre (or, at least, a responsivity-weighted mean radius), it is possible in principle to know the ionizing-photon flux on the clouds. However, as noted in Section 2, there is uncertainty in the radius given by reverberation mapping; so we considered two different radii, which give a range of a factor of four in ionizing photon fluxes. In running photoionization models the geometrical thickness h was assumed to be no larger than 10 light days. When the density is large (typically 10^9 cm^{-3} or greater), the computation was stopped when the temperature fell below 4000 K (the default stopping condition in CLOUDY), at which point there is little more optical emission.

As reviewed by Gaskell (2000), there is good evidence that the low- and high-ionization broad lines in an AGN are emitted from at least two separate (but quite possibly related) emission line regions. In this picture, Hβ is emitted mainly from a LIL region, which is commonly believed to be located in a disc, but the C IV and Lyα lines are from a HIL region, which is probably located above an accretion disc (Collin-Souffrin, 1986; Gaskell, 1988; 2000; Collin-Souffrin and Lasota, 1988). Snedden and Gaskell (2004a) have argued that both the high- and low-velocity emission of BLRs arises from predominantly optically thick clouds.

Reverberation mapping already tells us that the responsivity-weighted mean distances of the differing regions from the central ionizing source in 3C 390.3 and a few other well-studied sources are not very different[†]. The main difference between the conditions in the different

[†] The radial distributions are quite likely to be at least somewhat different, however.

emission line regions must therefore be in density. To compare the observed line ratios with the models, we assumed, for simplicity, that the lines were produced from the *same* gas clouds (*i.e.* a single component) and investigated how conditions vary with velocity. Since the relative contributions from the different regions change with velocity, we can infer differences in density in the two regions.

In Figure 4 we show the computed C IV, Lyα and Hβ line fluxes from individual clouds as a function of electron density (N_e) for different fluxes incident on the clouds. The intensity of the C IV line from a cloud decreases rapidly with increasing electron density above $N_e = 10^{10}\,\mathrm{cm}^{-3}$, while the Lyα and Hβ line intensities stay constant (this is a well-known effect due to the recombination of C^{3+} into C^{2+} as the ionization parameter decreases). From these line fluxes from individual clouds we next determined the line ratios from an ensemble of gas clouds spread over a range of radii. We considered three functional dependences of the covering factor on the distance r: $C \propto r^{-1}$, $C =$ constant and $C \propto r$. These correspond to different radial distributions of the gas. We assumed that the electron density was constant with distance.

In Figure 5 we show the integrated C IV-to-Lyα and Lyα-to-Hβ ratios versus the electron density for our three different radial dependences of the covering factors C for our high and low states. From comparison of the observed C IV-to-Lyα ratios (which, at the maximum of nuclear activity, can be seen to vary across the line profile over the range 0.6–2) and the computed C IV-to-Lyα ratios in Figure 5, we can see that these three differing covering factor behaviours all predict the observed changes in C IV-to-Lyα line ratios (decreasing ratio from the wings to the centre) by changing the electron density across the lines profiles in two ways:

(i) a density of about $10^7\,\mathrm{cm}^{-3}$ in the low-velocity core increasing to about $10^{10}\,\mathrm{cm}^{-3}$ in the higher-velocity wings or
(ii) a density of about $10^{13}\,\mathrm{cm}^{-3}$ in the low-velocity core decreasing to about $10^{12}\,\mathrm{cm}^{-3}$ in the higher-velocity wings.

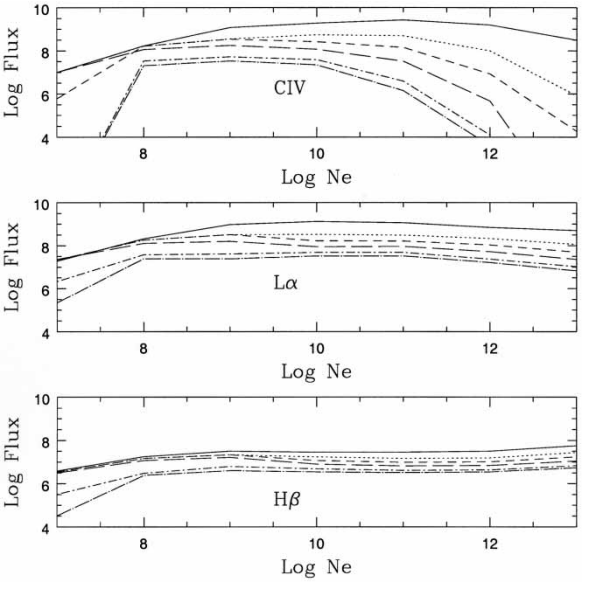

FIGURE 4 Line fluxes of C IV, Lyα and Hβ versus electron density, for different incident fluxes, for clouds illuminated by the central continuum: ———, $\log(\nu F_\nu) = 9.62$; · · · · · , $\log(\nu F_\nu) = 9.00$; - - - - - , $\log(\nu F_\nu) = 8.67$; - - - - - , $\log(\nu F_\nu) = 8.37$; – · – · –, $\log(\nu F_\nu) = 8.05$; – · – · –, $\log(\nu F_\nu) = 7.80$.

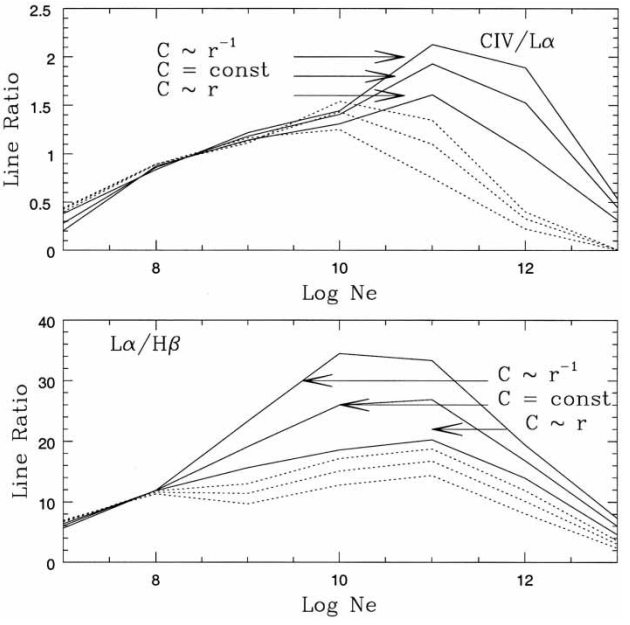

FIGURE 5 C IV-to-Lyα and Lyα-to-Hβ line ratios versus electron densities for different radial dependences of the covering factor C: ———, high state; · · · · · · , low state.

Of these two possibilities, the second is ruled out because the critical density of C III ($\lambda = 1909$ Å) is about $10^{9.5}$ cm^{-3}, and the profile of C III is similar to that of C IV. Thus the C IV-to-Lyα ratio in 3C 390.3 implies that the wings have a higher-density gas.

The change in the C IV-to-Lyα ratio with the changing continuum level also argues for the density increasing from about 10^7 cm^{-3} in the core to about 10^{10} cm^{-3} in the wings because the change in the ratio with luminosity is slight (compare Figures 3(a) and (b)), as is predicted by Figure 5. This would not be the case were the density about 10^{12} cm^{-3} because there would be a stronger change in the C IV-to-Lyα ratio.

As we have already mentioned, unlike the C IV-to-Lyα ratio, the Lyα-to-Hβ ratio is strongly affected by reddening. For a radio-loud FR II AGN such as 3C 390.3, Gaskell *et al*. (2004) find a typical reddening, $E(B-V)$ of the order of 0.3–0.7 magnitude or so. Using the flat nuclear reddening curve they find for radio-loud AGNs such as 3C 390.3 (see their Appendix 1), this implies that the Lyα-to-Hβ ratios in Figure 3 must be multiplied by a factor of about 2 to about 4. Failing to do this means that most of the Lyα-to-Hβ ratios in Figure 3 would fall too low on Figure 5 unless one went to extremely high densities and, as we have noted, very high densities are ruled out by C III]. With the sort of reddening correction suggested by Gaskell *et al*. (2004), the observed ratios fall well in the ranges calculated in Figure 5 for the likely range of densities.

Figure 3 shows that in both high and low states the Lyα-to-Hβ ratio is highest at low velocities and decreases at higher velocities. Despite the uncertainty in the reddening correction, Figure 5 implies that the only way to obtain this sort of behaviour is, again, if the density is about an order of magnitude higher for the gas emitting at a higher velocity. This could be accomplished with a density going from about 10^{10} cm s^{-3} at low velocities up to about 10^{12} cm s^{-3} at higher velocities.

While both the Lyα-to-Hβ and C IV-to-Lyα ratios give the interesting result that the density is higher in the higher-velocity gas, there is a discrepancy in the actual ranges of density.

This is because we have only taken a single component to represent two different cloud components. The different density ranges implied by the variation in line ratio with velocity can be reconciled, however, if we have two components, a LIL and a HIL.

5 DISCUSSION

The origin of the double-peaked lines in 3C 390.3 objects has been discussed for over two decades. Several models have been proposed to explain the double-peaked line profiles. They include an out-flowing biconical gas stream (Zheng *et al*., 1991), a binary black-hole system, each with an associated BLR (Gaskell, 1983; 1988; 1996), emission from a relativistic accretion disc (see for example Perez *et al*. (1988), Chen *et al*. (1989), and Dumont and Collin-Souffrin (1990)) and the photoionization by an anisotropic continuum source (Koratkar *et al*., 1996; Goad and Wanders, 1996).

Although each of these mechanisms could, in principle, produce asymmetric double-peaked profiles, each has problems. Eracleous *et al*. (1997) and Shapovalova *et al*. (2001) rejected the hypothesis of a binary black-hole system for 3C 390.3 as it implies black-hole masses too high to be reconciled with the observed spectral and variability properties. Gaskell and Snedden (1999) showed that the binary black-hole model is ruled out by line-variability data because the model predicts different lags for the red and blue displaced peaks. The biconical gas stream model also predicts a different response from the blue and the red wings of the broad emission lines to variability of the continuum and so is also ruled out by the short-term variability data. The outflowing biconical gas stream model also has a problem when the line profiles change asymmetry on longer time scales as the profiles go from a situation in which the blue peak is strongest to a situation in which the red peak is strongest (Oke, 1987; Veilleux and Zheng, 1991). Zheng (1996) found that, although the Lyα and C IV blue wings were usually stronger than the red wing for 3C 390.3 in the IUE archival data, there were a few epochs when the opposite was true. Gaskell (1996) has also shown that the blue peak in 3C 390.3 is gradually shifting in wavelength, which is again difficult to explain using a biconical outflow model. A contribution from at least *some* biconical outflow, however, is supported by spectropolarimetric observations showing structure in Hα (see for example Corbett *et al*. (2000)). The Goad–Wanders (1996) model with photoionization by an anisotropic continuum has similar difficulties to the biconical gas stream model. Variability also gives difficulties for a simple axially symmetric disc model (Gaskell, 1988; Gaskell and Snedden, 1999), but these difficulties can be overcome by invoking azimuthal structure. The independent variation in the red and blue wings in 3C 390.3 (and other objects) on long time scales requires the introductions of modifications in the model such as an orbiting hot spot (Zheng *et al*., 1991) or significant ellipticity (Eracleous *et al*., 1996).

Previous studies of the dependence of line ratios on velocity (see for example Snedden and Gaskell (2004a, b)) have looked at AGNs that do not show strong displaced peaks (*i.e.* not 3C 390.3 objects). The main result of our study here is that for 3C 390.3 the line ratios show *different dependences on velocity from those found for non-3C 390.3 objects*. There are two important differences:

(i) For 3C 390.3, the C IV-to-Lyα ratio *increases* as one goes to higher velocities (*i.e.* into the red and blue displaced peaks) while, for non-3C 390.3 objects, Snedden and Gaskell (2004b) found the C IV-to-Lyα ratio to be *independent of velocity*.
(ii) For 3C 390.3, the Lyα-to-Hβ line ratio *decreases* as one goes to higher velocities while, for non-3C390.3 objects, the ratio usually *increases* (Snedden and Gaskell, 2004b).

These differences strongly suggest that the physical conditions are different in the disc-like components of the lines. Our investigation suggests that the density is higher in the higher-velocity gas. From their study of Hα, Hβ and Lyα lines in a variety of non-3C 390.3 objects, Snedden and Gaskell (2004b) have found that the density is only slightly higher in the high-velocity gas. The densities that they infer are about 10^9–10^{10} cm^{-3}, which is why they find the opposite velocity-dependent behaviour of the Lyα-to-Hβ line ratio to the behaviour that we find for 3C 390.3 (see Figure 4).

Our photoionization modelling implies that the C IV-to-Lyα and Lyα-to-Hβ line ratios can be fitted with a two-component model which includes emission from two regions; a HIL and a LIL. We believe that the LIL is associated with the nuclear accretion disc and has a high electron density $N_e \approx 10^{11}$–10^{12} cm^{-3}, while the HIL is located in the lower-density ($N_e \approx 10^8$–10^{10} cm^{-3}), biconical outflow.

Obviously, both the HIL and the LIL regions are responding to changes in the central ionizing continuum. In Figure 2 the C IV and Lyα displaced peaks are clearly stronger at maximum light while the blue peak in the Hβ line is possibly somewhat more pronounced at minimum luminosity. The relative increase in prominence of the displaced peaks in C IV at maximum activity is readily explained if the density is high (10^{11} cm^{-3} or higher) because, at high densities (and hence low-ionization parameters), the C IV line flux is strongly sensitive to the ionizing continuum level, as can be seen in Figure 4. The Hβ line flux is less sensitive to the ionizing flux since the cloud is matter bounded.

6 CONCLUSIONS

Our main result is that the Lyα-to-Hβ ratio is high in the centre of the lines but decreases in the high-velocity wings for both high and low states of nuclear activity. This is the opposite to the trend seen in most other AGNs looked at so far. The C IV-to-Lyα ratio is low in the centre of the lines but becomes higher in the wings. This effect is especially clearly seen in the blue wing of the lines at the maximum of nuclear activity. This behaviour is, again, different from what is seen in other AGNs. We believe that the differences in the velocity dependences of the line ratios for 3C 390.3 compared with non-3C390.3 AGNs is due to the very prominent disc-like emission of 3C 390.3.

We have attempted to investigate the velocity dependence of physical conditions by using the photoionization code CLOUDY. The behaviour of the line ratios is consistent with the fact that the density is higher in the higher-velocity gas. We believe that the emission in the lines can be reproduced approximately by using two components:

(i) a high-density component ($N_e = 10^{11}$–10^{12} cm^{-3}) with a double-peaked profile which particularly contributes to the Balmer lines;
(ii) a lower-density component ($N_e = 10^8$–10^{10} cm^{-3}), contributing mainly to the HIL emission.

We identify the first of these with a disc-like component, and the second with a component above the disc.

Acknowledgements

We are grateful to Elizabeth Klimek for her help in the preparation of this paper, and to Vladimir Pronik for useful comments. L.N. and N.B, acknowledge support under RFFI Grant 00-02-16272; MG acknowledges support by the US National Science Foundation through Grant

AST 03-07912, and by the Space Telescope Science Institute though Grants AR-05796.01-94 and AR-09926.01. The Space Telescope Science Institute is operated by AURA, Inc., under National Aeronautics and Space Administration contract NAS5-26555.

References

Antokhin, I. I. and Bochkarev, N. G. (1983) *Soviet Astron.* **27**, 261.
Blandford, R. D. and McKee, C. F. (1982) *Astrophys. J.* **255**, 419.
Bochkarev, N. G. and Pudenko, S. P. (1975) *Soviet Astron. Lett.* **1**, 53.
Chen, K., Halpern, J. P. and Filippenko, A. V. (1989) *Astrphys. J.* **339**, 742.
Collin-Souffrin, S. (1986) *Astron. Astrophys.* **166**, 115.
Collin-Souffrin, S., Dyson, J. E., McDowell, J. C. and Perry, J. J. (1988) *Mon. Not. R. Astron. Soc.* **232**, 539.
Collin-Souffrin, S. and Lasota, J.-P. (1988) *Publs. Astron. Soc. Pacif.* **100**, 1041.
Corbett, E., Robinson, A., Axon, D.J., Young and Hough, J.H. (2000) *Mon. Not. R. Astron. Soc.* **319**, 685.
Dietrich, M., *et al.* (1998) *Astrophys. J., Suppl. Ser.* **115**, 185.
Dumont, A.-M. and Collin-Souffrin, S. (1990) *Astron. Astrophys.* **229**, 313.
Dumont, A.-M., Collin-Souffrin, S. and Nazarova, L. S. (1998) *Astron. Astrophys.* **311**, 11.
Eracleous, M., Halpern, J. P. and Livio, M. (1996) *Astrophys. J.* **459**, 89.
Eracleous, M., Halpern, J. P., Gilbert, A. M., Newman, J. A. and Filippenko, A. V. (1997) *Astrophys. J.* **490**, 216.
Ferland, G. J. *et al.* (2004) Internal Report, Department of Physics and Astronomy, University of Kentucky, Lexington, Kentucky, USA.
Ferland, G. J. Korista, K. T., Verner, D. A., Ferguson, J. W., Kingdon, J. B. and Verner, E. M. (1998) *Publs. Astron. Soc. Pacif.* **110**, 761.
Gaskell, C. M. (1983) In: *Quasars and Gravitational Lenses Proceedings of the 24th Liege International Astrophysics Colloquim* (Cointe-Ougree: University of Liege), p. 471
Gaskell, C. M. (1988) In: H. R. Miller and P. J. Wiita (eds), *Active Galactic Nuclei*, Springer, Berlin, p. 61.
Gaskell, C. M. (1996) *Astronphys. J.* **464**, L107.
Gaskell, C. M. (2000) *New Astron. Rev.* **44**, 563.
Gaskell, C. M., Goosmann, R. W., Antonucci, R. R. J. and Whysong, D. H. (2004) *Astrophys. J.* (in press).
Gaskell, C. M. and Snedden, S. A. (1999) In: C. M. Gaskell *et al.* (eds), *Structure and Kinematics of Quasar Broad-Line Regions*, Vol. 175 ASP Conference Series (San Francisco: Astronomical Society Pacific), p. 157.
Goad, M. and Wanders, I. (1996) *Astrophys. J.* **469**, 113.
Grandi, P., *et al.* (1999) *Astron. Astrophys.* **343**, 33.
Koratkar, A., *et al.* (1996) *Astrophys. J.* **470**, 378.
Matthews, W. G. and Ferland, G. J. (1987) *Astrophys. J.* **323**, 456.
Livio, M. and Xu, C. (1997) *Astrophys. J.* **478**, L63.
O'Brien, P. T., *et al.* (1998) *Astrophys. J.* **509**, 1630.
O'Brien, P. T. (1998) *Observatory* **118**, 3370.
Oke, J. B. (1987) In: J. A. Zensus and T. J. Pearson (eds), *Superluminal Radio Sources*, Cambridge University Press, Cambridge, p. 267.
Perez, E., Penston, M. V., Tadhunter, C., Mediavilla, E. and Moles, M. (1988) *Mon. Not. R. Astron. Soc.* **230**, 353.
Sandage, A. R. (1966) *Astrophys. J.* **334**, 95.
Sergeev, S. G., Pronik, V. I., Peterson, B. M., Sergeeva, E. A. and Zheng, W. (2002) *Astrophys. J.* **576**, 660.
Shapovalova, A. I., Chavushyan, V. H, Carrasconst, L., *et al*. (2001) *Astron. Astrophys.* **376**, 775.
Snedden, S. A. (2001) PhD Thesis, University of Nebraska, Nebraska, USA.
Snedden, S. A. and Gaskell, C. M. (2004a) *Astrophys. J.* (in press).
Snedden, S. A. and Gaskell, C. M. (2004b) *Astrophys. J.* (submitted).
Veilleux, S. and Zheng, W. (1991) *Astrophys. J.* **377**, 89.
Wamsteker, W., Ting-gui W., Schartel, N. and Vio, R. (1997) *Mon. Not. R. Astron. Soc.* **288**, 225.
Zheng, W., Veilleux, S. and Grandi, S. A. (1991) *Astron. J.* **381**, 411.
Zheng, W. (1996) *Astron. J.* **111**, 1498.